mortality, because LRI is an acute disease. The projected secular trend of LRI mortality in SSA is declining, mainly because of expectations of improved access to clinical case management using antibiotics (*29*). Therefore rapid transitions to cleaner fuels promptly save lives when the background rates are at their worst (i.e., in the early part of the projection period). Second, rapid transition to cleaner fuels also reduces adult female deaths from COPD significantly. Because COPD is a chronic disease, the health benefits of cleaner fuels accrue gradually over time (fig. S10). With rapid transitions to clean fuels, a larger number of adult women will witness complete benefits by 2030. Coupled with the increasing number of older women in Africa because of population growth and aging (*30*), the benefits of rapid transition in reducing COPD are amplified in the later part of the projection period.

18. These are reductions in particulate matter, which is the pollutant consistently associated with the most substantial negative health impacts (*31*). Carbon monoxide (CO) is also a harmful pollutant associated with biomass fuels. In measurements in Kenya, CO concentrations from charcoal were not significantly different from those from wood stoves (*31*). Promoting charcoal as a household fuel should be accompanied with education about safe practices.
19. In practice, a large number of future energy paths may be taken. Examples include transitions to improved ceramic wood stoves among wood users and to mixed fossil and biomass fuels among biomass users. Because ceramic stove and mixed-fuel use are less precisely defined alternatives, both interventions have substantial heterogeneity in health hazards. Under a specific definition, gradual and rapid transitions to ceramic wood stoves would avoid 400,000 and 1.2 million deaths, respectively; gradual and rapid transitions to mixed fossil and biomass fuels would avoid 900,000 and 2.8 million deaths. Well-designed and well-maintained ventilated stoves with chimneys may provide health benefits that are comparable to those from charcoal, but they have not been widely disseminated in Africa.
20. The cost of cooking with wood is highly variable because wood can be obtained for free, although in urban areas this not usually the case. Market prices for split fuel wood (*26*) indicate that annual cooking costs would be at least $200 if all wood were purchased. For comparison, using a combination of field observations and fuel prices reported in (*26*), we estimate a range of annual cooking costs for charcoal ($116 to $271), kerosene ($149 to $273), LPG ($274 to $374), and electricity ($230 to $467). The range in costs is a function of fuel prices, which depend on the quantity purchased, the cost of the stove (amortized over its expected lifetime using a 12% discount rate), and stove efficiencies [reported, for example, in (*32*)].
21. Estimates of child deaths that could have been avoided worldwide in 2000 if the coverage of a number of nutritional, environmental, and treatment interventions were increased to 99% of children at need show that various interventions ranged between 1 and >10% (*33*). Interventions with particularly large benefits include oral rehydration therapy, insecticide-treated bed nets, clean water and sanitation, antibiotics for treating pneumonia, micronutrient supplementation, and exclusive breastfeeding (*33*). If the same assumption of 99% coverage is applied, in 2000, charcoal (99% of current wood users switching to charcoal) would save 250,000 childhood LRI deaths (6% of all SSA child deaths) and petroleum-based fossil fuels (99% of all biomass users) would save 350,000 childhood LRI deaths (8% of all SSA child deaths).
22. K. R. Smith *et al.*, *Greenhouse Gases from Small-Scale Combustion in Developing Countries: Charcoal Kilns in Thailand* [Technical Report No. EPA-600/R-99-109, U. S. Environmental Protection Agency (EPA), Washington, DC, 1999].
23. O. C. Ferreira, *Economy and Energy* **20** (May-June 2000).
24. Charcoal can be made from many forms of biomass, including agricultural and timber-processing residues. There are some attempts to market such products in several countries in SSA, but market penetration is currently very low.
25. Government of India, *Census of India: 2001* (Central Statistical Office, Delhi, 2001).
26. Ministry of Energy (Kenya), *Study on Kenya's Energy Demand, Supply and Policy Strategy for Households, Small Scale Industries and Service Establishments: Final Report* (KAMFOR Company Limited, Nairobi, 2002).
27. E. Boy, N. Bruce, H. Delgado, *Environ. Health Perspect.* **110**, 109 (2002).
28. V. Mishra, X. Dai, K. R. Smith, L. Mika, *Ann. Epidemiol.* **14**, 740 (2004).
29. C. J. L. Murray, A. D. Lopez, in *The Global Burden of Disease*, C. J. L. Murray, A. D. Lopez, Eds. (Harvard School of Public Health on behalf of WHO and World Bank, Boston, 1996), pp. 325–395.
30. UN, *World Population Prospects: The 2002 Revision* (Population Division of the Department of Economic and Social Affairs of the UN Secretariat, 2004) available at www.un.org/popin/data.html.
31. M. Ezzati, B. Mbinda, D. Kammen, *Environ. Sci. Technol.* **34**, 578 (2000).
32. K. R. Smith *et al.*, *Greenhouse Gases From Small-Scale Combustion Devices in Developing Countries Phase IIa: Household Stoves in India* (Technical Report No. EPA-600/R-00-052, EPA, Washington, DC, 2000) available at: www.teriin.org/climate/emission.htm.
33. G. Jones *et al.*, *Lancet* **362**, 65 (2003).
34. This research was supported by the EPA Office of Atmospheric Programs, the Energy Foundation, and NIH (grant PO1-AG17625). The authors thank B. H. Singer for comments on early drafts of this article; K. R. Smith and D. M. Pennise for discussions on GHG methods; and R. E. Black, A. D. Lopez, and E. K. Mulholland for discussions on mortality and mortality projections.

Supporting Online Material
www.sciencemag.org/cgi/content/full/308/5718/98/DC1
Materials and Methods
Figs. S1 to S11
Tables S1 to S7
References

28 October 2004; accepted 10 February 2005
10.1126/science.1106881

A Late Jurassic Digging Mammal and Early Mammalian Diversification

Zhe-Xi Luo* and John R. Wible

A fossil mammal from the Late Jurassic Morrison Formation, Colorado, has highly specialized teeth similar to those of xenarthran and tubulidentate placental mammals and different from the generalized insectivorous or omnivorous dentitions of other Jurassic mammals. It has many forelimb features specialized for digging, and its lumbar vertebrae show xenarthrous articulations. Parsimony analysis suggests that this fossil represents a separate basal mammalian lineage with some dental and vertebral convergences to those of modern xenarthran placentals, and reveals a previously unknown ecomorph of early mammals.

The Late Jurassic was a time of rapid diversification of mammals. Insectivorous eutriconodontans, symmetrodontans, and dryolestoids, and the omnivorous multituberculates dominated the Late Jurassic mammalian faunas of Laurasia, displacing several more primitive mammaliaform lineages (*1*–*3*). Most mammals of the Jurassic and Early Cretaceous with preserved skeletal elements are generalized terrestrial mammals (*4*–*7*), except docodontans (*2*). Here, we report a new mammal with dental specializations like those known only from early Tertiary palaeanodonts and extant xenarthran and tubulidentate placental mammals, in addition to numerous fossorial (digging) skeletal features.

Carnegie Museum of Natural History, Pittsburgh, PA 15213, USA.

*To whom correspondence should be addressed. E-mail: luoz@carnegiemnh.org

Fruitafossor windscheffeli gen. et sp. nov. (*8*) is represented by relatively complete lower jaws (Fig. 1), incomplete cranium, and nearly 40% of the postcranial skeleton, including complete forelimb and manus (Fig. 2), several elements of the hindlimb and hindfoot (pes) (Fig. 3), and most of the thoracic, complete lumbar and sacral, and some caudal vertebrae. The new taxon is distinguishable from all known Mesozoic mammaliaforms in having tubular and single-rooted molars with open-ended roots (Fig. 1) and in that the molar crown lacks enamel. It differs from all known Mesozoic mammaliaforms in that the posterior opening of the mandibular canal is located anterior to the pterygoid crest in a broad meckelian groove. It differs from all Jurassic mammals (except *Hadrocodium*) (*9*) in having an inflected mandibular angle that is continuous with the pterygoid crest (Fig. 1). *Fruitafossor* is also distinguishable from and more primitive than the well-established and successively more inclusive hierarchies of eutherians (*10*, *11*), the crown therian clade of eutherians and metatherians (*7*, *12*, *13*), the trechnotherian clade (*Zhangheotherium* and crown therians) (*14*–*17*), and the theriiform clade (multituberculates and trechnotherians) (*18*), and is more plesiomorphic (*19*, *20*) than each of these clades by many characteristics.

The most prominent feature of *Fruitafossor* is its single- and open-rooted tubular molars with elliptical cross section, which suggests that the molars had a sustained and continuous growth in life and are similar to the teeth of extant armadillos (dasypodids), which feed primarily on insects and small invertebrates, supplemented with plants (*21*). We thus infer that *Fruitafossor* had a similar diet. Tubular molars of *Fruitafossor* also bear some resemblance to the living aardvark (*Orycteropus*) that is specialized for feeding on ants and termites, although some aardvark teeth are bilobed. Among early Tertiary mammals, palaeanodonts also developed similar (although fewer) single-rooted cheek teeth with elliptical cross section.

Fruitafossor was a fossorial mammal, with forelimb and manual structures for scratch digging (*22*, *23*) (Fig. 2). The scapular glenoid is saddle-shaped and formed by both the scapula and a separate coracoid. This suggests that the range of mobility of the shoulder joint was similar to that of monotremes, rather than that of moles. The large infraspinous fossa occupies much of the lateral aspect of the scapula, and the incipient supraspinous fossa is represented by a small area on the cranial border of the scapula. The acromion is platelike and forms a rigid articulation with the clavicle. The scapula is similar to those of monotremes (Fig. 3), *Morganucodon*, and *Haldanodon* in most characteristics. The humerus (Fig. 2) has a large deltopectoral crest and a hypertrophied tuberosity for the insertion of a large teres muscle that also has an extensive area of origination from the prominent posteroventral angle of the scapula. The distal portion of the humerus is very wide with well-developed epicondyles. The ectepicondyle has a hypertrophied supinator/extensor crest typical of small digging mammals (*22*, *23*). The ratio of epicondylar width to humeral length is about 65%, above the average of all extant fossorial mammals in this index (*22*). The ulna has an elongate and medially pointed olecranon process, presumably for very large triceps, dorsoepitrochlearis, and digital flexor muscles. The olecranon length is 66% that of the ulnar portion anterior to the semilunar notch, also above the average of all extant fossorial mammals (*22*).

The manus has only four digits. The carpals are all proximo-distally shortened, as are metacarpals 2 to 4 and phalanges of digits 2 to 4. The proximal phalanges of digits 2 and 3 are the shortest. However, metacarpal 1 and digit 1 phalanges are more gracile than the short and blocklike metacarpals and phalanges of digits 2, 3, and 4. The terminal (claw-bearing) phalanx is the longest on each digit; it has a large flexor tubercle. The distal portion of the terminal phalanx is dorso-ventrally flat, broad, and nearly spatulate, although its apex is not bifid. A very large sesamoid bone for the digital flexor muscle is present on the plantar aspect of the manus, and a single sesamoid is also present ventral to the metacarpophalangeal joint (Fig. 2). Shortened and robust metacarpals and phalanges, the proportion of phalanges within the digit (*22*), and the main features of the terminal phalanx (*24*) are all typical of fossorial mammals.

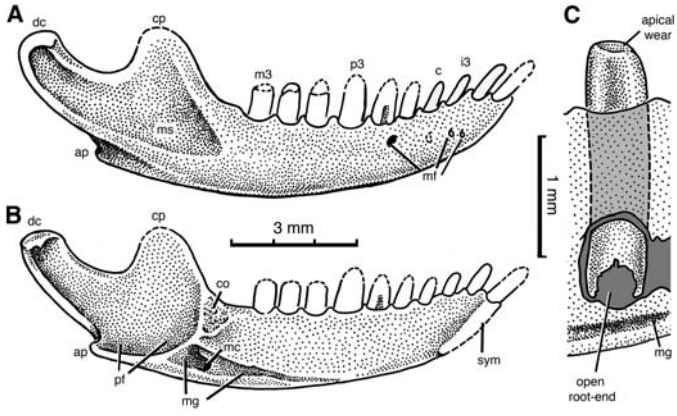

Fig. 1. *Fruitafossor windsheffeli* gen et sp. nov. (Holotype: LACM 150948): Reconstruction of left mandible and lower dentition (i3, c1, p3, m3) in (**A**) lateral and (**B**) medial views. (**C**) Tubular lower molar (m1) in medial view with open root-end exposed in the broken mandible [tubular structure of the molar is also corroborated by computerized tomography (CT) scans]. Abbreviations: ap, inflected angular process; co, facet for coronoid bone; cp, coronoid process; dc, dentary condyle; mc, posterior opening of mandibular canal; mf, anterior mental foramina; mg, meckelian groove; ms, masseteric fossa; pf, pterygoid fossa; sym, mandibular symphysis.

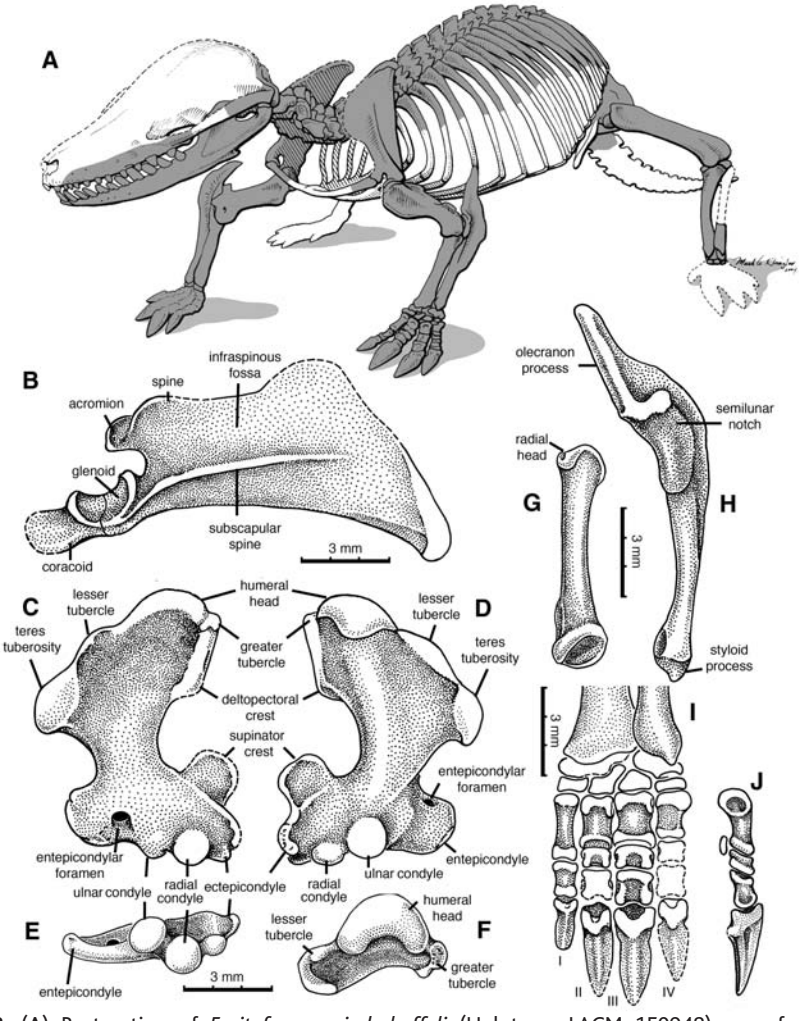

Fig. 2. (**A**) Restoration of *Fruitafossor windscheffeli* (Holotype: LACM 150948) as a fossorial mammal with forelimb and manual features for scratch digging and a dentition specialized for feeding on termites, other insects, and supplemented with plants (shaded parts of the skeleton are preserved in the type specimen); (**B**) left scapula in ventrolateral (tilted "posterolateral") view; (**C** to **F**) left humerus in ventral ("anterior"), dorsal ("posterior"), distal, and anteromedial views; (**G**) posteromedial view of left radius; (**H**) anterior view of left ulna; (**I**) plantar (ventral) view of left manus; and (**J**) lateral view of metacarpal and phalanges of digit 3.

However, many manual and digital features are also unique to *Fruitafossor*. The new taxon is distinctive from monotremes in the width-length proportion of metacarpal 1, which has nearly the same broad width as that of other metacarpals. Its short and broad metacarpals and phalanges differ from the gracile metacarpals and phalanges of eutriconodonts (*7*, *25*), multituberculates (*26*, *27*), and trechnotherians (*5*, *28*–*30*), which have less specialized terrestrial and other locomotory adaptations. The absence of a bifid claw differs from many (but not all) Cenozoic and extant placental mammals with digging adaptations (*22*, *23*).

Fruitafossor is characterized by a mixture of many plesiomorphies of premammalian mammaliaforms, a large number of eutriconodontan-like and monotreme-like features that are typical of basal mammals, and some derived features of tubulidentate and xenarthran placentals. Most of the scapular features are plesiomorphic and similar to those of morganucodontids, *Haldanodon*, and living monotremes (Fig. 3). The humerus lacks a distinctive humeral head but has a broad intertubercular groove; the two distal humeral condyles for the radius and ulna are spherical, widely separated, and arranged obliquely. In these features of the humerus, *F. windscheffeli* is similar to tritylodontids (*31*), tritheledontids (*32*), and morganuocodontids (*4*).

Fruitafossor shares plesiomorphic carpal features with eutriconodontans, multituberculates, and *Zhangheotherium* in the proportion of the hamate, lunate, and scaphoid, and lacks the derived features of the hypertrophied hamate

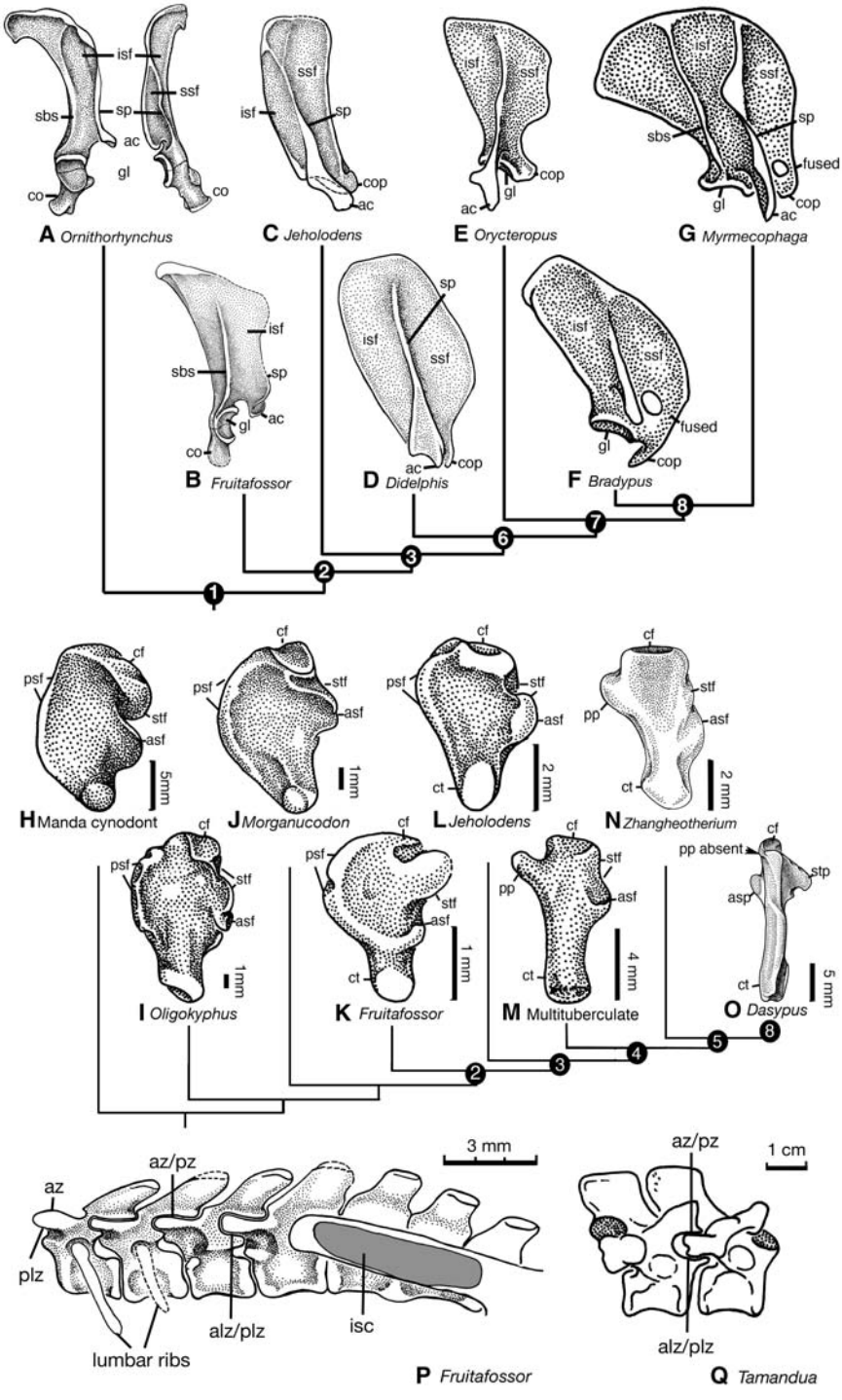

Fig. 3. Comparison of *Fruitafossor* with other mammals and premammalian cynodonts. (Top) Right scapulae of (**A**) monotreme *Ornithorhynchus* (platypus, lateral and anterior views); (**B**) basal mammal *Fruitafossor* (ventrolateral view); (**C**) eutriconodontan *Jeholodens* (lateral view); (**D**) marsupial *Didelphis* (opossum, lateral view); (**E**) placental *Orycteropus* (aardvark, lateral view); (**F**) placental *Bradypus* (sloth, ventral or plantar view); and (**G**) placental *Myrmecophaga* (giant anteater, lateral view). Abbreviations: ac, acromion process; co, coracoid bone; cop; coracoid process (reduced coracoid bone fused to scapula); gl, scapular glenoid joint surface; isf, infraspinous fossa; sbs, subscapular spine; sp, scapular spine; ssf, supraspinous fossa. (Middle) Calcanei (right, all in ventral view) of (**H**) the Manda cynodont; (**I**) mammaliamorph *Oligokyphus*; (**J**) mammaliaform *Morganucodon*; (**K**) *Fruitafossor*; (**L**) eutriconodontan *Jeholodens*; (**M**) a Late Cretaceous multituberculate; (**N**) trechnotherian *Zhangheotherium*; and (**O**) placental *Dasypus* (armadillo). [(H), (I), and (J) are redrawn from (*12*).] (Bottom) (**P**) Lumbars, mobile lumbar ribs, and sacral region of *Fruitafossor*. (**Q**) Lumbar vertebrae of placental *Tamandua* [after (*34*)]. Abbreviations: asf, astragalar facet; asp, astraglar process (astragalar facet is on the dorso-medial aspect of this process); alz/plz, lateral zygapophyseal vertebral articulation (derived xenarthran condition); az, prezygapophysis; az/pz, primitive mammalian zygapophyseal articulation; cf, calcaneocuboid facet; ct, calcaneal tuber; isc, ilio-sacral contact; pp, peroneal process; psf, peroneal shelf; stf, vertically oriented sustentacular facet; stp, sustentacular process (the horizontally oriented sustentacular facet is on the dorsal aspect of this process). Node (1) Crown Mammalia; Node (2) clade defined by common ancestor of *Fruitafossor* and crown Theria; Node (3) clade defined by ancestor of *Jeholodens* and crown Theria: enlargement of supraspinous fossa; acromial process extending beyond the glenoid; glenoid uniformly concave (not saddle-shaped); Node (4) Theriiformes, with synapomorphies of distinctive peroneal process (instead of a broad peroneal shelf), elongation of calcaneal tuber; Node (5) Trechnotherians; Node (6) Crown Theria with synapomorphies of shelflike sustentacular structure and a partial dorsal placement of sustentacular facet (instead of a medial placement); Node (7) Crown placental synapomorphy: loss of peroneal process or shelf; Node (8) Xenarthra: coracoid process fused with cranial border of scapula.

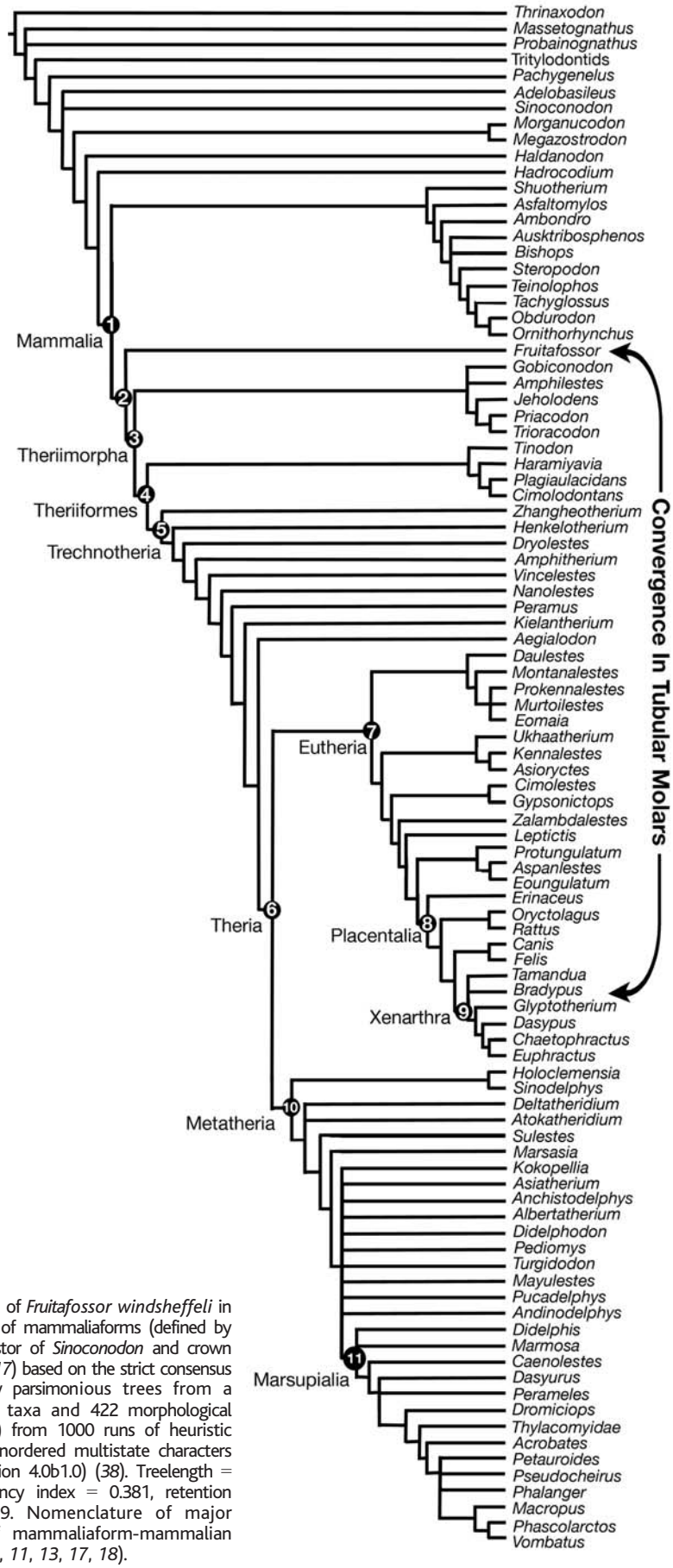

Fig. 4. Position of *Fruitafossor windsheffeli* in the phylogeny of mammaliaforms (defined by common ancestor of *Sinoconodon* and crown mammals) (*3*, *17*) based on the strict consensus of 184 equally parsimonious trees from a matrix of 96 taxa and 422 morphological characters (*20*) from 1000 runs of heuristic search, with unordered multistate characters by PAUP (version 4.0b1.0) (*38*). Treelength = 2111, consistency index = 0.381, retention index = 0.789. Nomenclature of major hierarchies of mammaliaform-mammalian clades after (*7*, *11*, *13*, *17*, *18*).

of metatherians or the enlarged trapezium of eutherians (*7*, *11*, *12*). The exposed portion of the scapula is similar to that of docodontans (*2*). Its calcaneus, although autapomorphic in some regards, bears strong similarities to those of *Morganucodon* and tritylodontids (*4*, *12*) and is far more primitive than the calcanei of multituberculates (*26*, *27*), *Zhangheotherium* (*29*), metatherians, and eutherians (*7*, *11*) (Fig. 3). Its lumbar vertebrae bear unfused and mobile lumbar ribs down to the penultimate lumbar vertebra (Fig. 3P), a feature of cynodonts (*31*) and monotremes.

Fruitafossor is similar to eutriconodontans and some spalacotheriid symmetrodontans in the rounded posteroventral margin of the mandible that is continuous with the dentary condyle (Fig. 1). The medial side of the mandible has a distinctive pterygoid fossa, a plesiomorphic feature of many other Late Jurassic mammals. However, the mandible has an anteriorly placed and inflected angle. The posterior opening of the mandibular canal is placed in a very broad meckelian groove, and anterior to the pterygoid fossa. These features are not known for any Jurassic and Cretaceous mammals and are autapomorphic for this new mammalian lineage.

Fruitafossor is similar to tubulidentates (aardvark) and armadillos (dasypodids) in its tubular molars, each with a single and open root (Fig. 1). Its lumbar vertebrae have a lateral anterior- and posterior-zygapophyseal articulation, in addition to the typical pre- and postzygapophyseal intervertebral articulations of most mammals (Fig. 3, P and Q). These are similar to the xenarthrous thoracic and lumbar vertebrae that are otherwise unique features for the placental order of Xenarthra (sloths, anteaters, and armadillos) (*33*, *34*). Given that *Fruitafossor* is not closely related to xenarthrans (Fig. 4), it must have independently developed this type of intervertebral articulation, including the anterior and posterior lateral zygapophyseal joints.

Fruitafossor differs from tubulidentates and armadillos in a long list of osteological characters (*20*). The presence of a broad meckelian groove indicates that the middle ear bones were still connected with the lower jaw in *Fruitafossor*. The round posterior margin of the mandible is different from the posteriorly positioned angle of most placentals, including aardvarks, sloths, and armadillos. *Fruitafossor* lacks the fusion of proximal caudal vertebrae with the sacral vertebrae, and the fusion of ischium with the caudals that are important apomorphies of xenarthrans. The medially placed sustentacular and astragalar facets, as well as the broad peroneal shelf on the calcaneus, indicate that *Fruitafossor* lacked the superpositional relationships of the calcaneus and astragalus of modern placentals. No trechnotherian mammals (including marsupials and placentals) have any of the primitive characteristics of the forelimbs seen in *Fruitafossor*.

We incorporated the dental and vertebral similarities of *Fruitafossor*, tubulidentates, and xenarthrans into global parsimony analysis of morphological features known for Mesozoic mammals and the major groups of extant mammals (*3*, *7*, *17*). *Fruitafossor* is resolved to be a basal mammal emerging in the Late Jurassic mammalian diversification and has no closer relationship to placental xenarthrans than have other nonplacental trechnotherians (Fig. 4), and is not a eutherian, let alone a xenarthran.

Xenarthrous intervertebral articulations help the vertebral column resist torsion produced by digging (*35*). We suggest that the open and single-rooted tubular molars and the xenarthrous lumbar vertebrae in *Fruitafossor* are convergent features to those of some modern placentals. So that it should not be misconstrued, we emphasize that *Fruitafossor* is not related to modern placental xenarthrans and has no bearing on the timing of divergence of xenarthran placentals (*36*, *37*).

References and Notes

1. G. G. Simpson, *Mem. Peabody Mus. Yale Univ.* **3**, 1 (1929).
2. T. Martin, B. Krebs, Eds., *Guimarota: A Jurassic Ecosystem* (Verlag Dr. Friedrich Pfeil, Munich, 2000).
3. Z. Kielan-Jaworowska, R. L. Cifelli, Z.-X. Luo, *Mammals from the Age of Dinosaurs: Origins, Evolution and Structure* (Columbia Univ. Press, New York, 2004).
4. F. A. Jenkins Jr., F. R. Parrington, *Philos. Trans. R. Soc. London* **273**, 387 (1976).
5. Y.-M. Hu, Y.-Q. Wang, C.-K. Li, Z.-X. Luo, *Vertebr. PalAsiat.* **36**, 102 (1998).
6. A. Weil, *Nature* **416**, 798 (2002).
7. Z.-X. Luo, Q. Ji, J. R. Wible, C.-X. Yuan, *Science* **302**, 1934 (2003).
8. Etymology: "*Fruita*," for provenance of this new mammal near the town of Fruita, Colorado; "*- fossor*," after the fossorial (digging) specialization of the forelimbs and vertebrae; the specific name "*windscheffeli*" is in honor of Wally Windscheffel, who discovered the holotype specimen. Systematics: Class Mammalia, Order and Family *incertae sedis*, Genus et Species nov. *Fruitafossor windscheffeli*. Holotype: Natural History Museum of Los Angeles County (LACM) 150948 (Figs. 1 and 2), an individual represented by lower jaws, incomplete cranium, and about 40% of the postcranial skeleton. Locality and age: the Fruita Paleontology Area, Fruita, Colorado, USA; mudstones of the Morrison Formation, Kimmeridgian, about 150 million years (ma).
9. Z.-X. Luo, A. W. Crompton, A.-L. Sun, *Science* **292**, 1535 (2001).
10. M. J. Novacek *et al.*, *Nature* **389**, 483 (1997).
11. Q. Ji *et al.*, *Nature* **416**, 816 (2002).
12. F. S. Szalay, *Evolutionary History of the Marsupials and an Analysis of Osteological Characters* (Cambridge Univ. Press, Cambridge, 1994).
13. G. W. Rougier, J. R. Wible, M. J. Novacek, *Nature* **396**, 459 (1998).
14. D. R. Prothero, *Bull. Am. Mus. Nat. Hist.* **167**, 277 (1981).
15. Y.-M. Hu, Y.-Q. Wang, Z.-X. Luo, C.-K. Li, *Nature* **390**, 137 (1997).
16. M. C. McKenna, S. K. Bell, *Classification of Mammals above the Species Level* (Columbia Univ. Press, New York, 1997).
17. Z.-X. Luo, Z. Kielan-Jaworowska, R. L. Cifelli, *Acta Palaeontol. Pol.* **47**, 1 (2002).
18. T. B. Rowe, *J. Vertebr. Paleontol.* **8**, 241 (1988).
19. Diagnosis. Lower dentition: i3, c1, p3, m3. Upper dentition: I?, C1, P3, M3. Differs from all known Mesozoic mammaliaforms and most Cenozoic mammals (except some xenarthans and tubulidentates) in molars with a single and open-ended root and without enamel. Differs from all known mammaliaforms (except xenarthrans) in having an extra ("xenarthrous") articulation between lumbar vertebrae. More derived than most mammaliaforms in lacking the medial ridge above the postdentary trough and in the presence of a medial pterygoid fossa on the mandible. Distinguishable from multituberculates, eutriconodontans, and spalacotheriids in having a mandibular angle. Differs from mammaliaforms (except *Hadrocodium*) and Jurassic and Cretaceous cladotherians (except *Montanalestes* and metatherians) in the inflection of this angle. Differs from monotremes in the absence of a deeply excavated masseteric fossa, in having gracile metacarpal and phalanges of digit 1, and in the absence of the parafibular process of the fibula. Differs from all Cenozoic fossil therians (including palaeanodonts) and extant placentals (including tubulidentates and xenarthrans) in retaining a long list of plesiomorphies [full differential diagnosis in (*20*)].
20. Supporting material is available on *Science* Online.
21. R. M. Nowak, J. L. Paradiso, *Walker's Mammals of the World* (Johns Hopkins Univ. Press, Baltimore, MD, ed. 4, 1983).
22. M. Hildebrand, in *Functional Vertebrate Morphology*, M. Hildebrand, D. M. Bramble, K. F. Liem, D. B. Wake, Eds. (Belknap, Cambridge, MA, 1985), pp. 89–109.
23. K. D. Rose, in *Encyclopedia of Paleontology*, R. Singer, Ed. (Fitzroy Dearborn, Chicago and London, 1999), vol. 1, pp. 220–226.
24. N. McLeod, K. D. Rose, *Am. J. Sci.* **293**, 300 (1993).
25. Q. Ji, Z.-X. Luo, S.-A. Ji, *Nature* **398**, 326 (1999).
26. D. W. Krause, F. A. Jenkins, *Bull. Mus. Comp. Zool.* **150**, 199 (1983).
27. Z. Kielan-Jaworowska, P. P. Gambaryan, *Fossils Strata* **36**, 1 (1994).
28. G. W. Rougier, Q. Ji, M. J. Novacek, *Acta Geol. Sin.* **77**, 7 (2003).
29. Z.-X. Luo, Q. Ji, *J. Mamm. Evol.*, in press.
30. B. Krebs, *Berl. Geowiss. Abh.* **A133**, 1 (1991).
31. H.-D. Sues, thesis, Harvard University (1983).
32. C. E. Gow, *Palaeontol. Afr.* **37**, 93 (2001).
33. K. D. Rose, R. J. Emry, in *Mammal Phylogeny: Placentals*, F. S. Szalay, M. J. Novacek, M. C. McKenna, Eds. (Springer, Berlin, 1993), pp. 81–101.
34. T. J. Gaudin, *Fieldiana (Geol. New Ser.)* **41**, 1 (1999).
35. T. J. Gaudin, A. A. Biewener, *J. Morphol.* **214**, 63 (1992).
36. S. Kumar, S. B. Hedges, *Nature* **392**, 917 (1998).
37. W. J. Murphy *et al.*, *Science* **294**, 2348 (2001).
38. D. L. Swofford, *PAUP*: Phylogenetic Analysis Using Parsimony (and Other Methods)*, version 4.0b1.0 (Sinauer, Sunderland, MA, 2000).

39. We thank W. Windscheffel and C. Safris for discovering this fossil; W. Windscheffel and A. Henrici for preparation; T. Ryan and A. Grader for access to the CT Scanning Facility at the Pennsylvania State University; G. Callison and the Grand Junction office of the Bureau of Land Management for support; T. Gaudin, T. Martin, and J. Rawlins for numerous discussions; S. McLeod, X.-M. Wang, and L. Chiappe for access to research collections; anonymous reviewers for their improvement of the manuscript; and M. Klingler for illustrating Fig. 2A. Supported by NSF (USA) and Carnegie Museum (Z-X.L. and J.R.W.), National Geographic Society (USA), and National Natural Science Foundation (China) (Z.-X.L.).

Supporting Online Material

www.sciencemag.org/cgi/content/full/308/5718/103/DC1
SOM Text
Matrix S1
PAUP Search Results
References
Movies S1 and S2

20 December 2004; accepted 7 February 2005
10.1126/science.1108875

Comparison of Fine-Scale Recombination Rates in Humans and Chimpanzees

Wendy Winckler,[1,3,5]* Simon R. Myers,[6]* Daniel J. Richter,[5] Robert C. Onofrio,[5] Gavin J. McDonald,[1,5] Ronald E. Bontrop,[7] Gilean A. T. McVean,[6] Stacey B. Gabriel,[5] David Reich,[3,5] Peter Donnelly,[6]†,‡ David Altshuler[1–5]†,‡

We compared fine-scale recombination rates at orthologous loci in humans and chimpanzees by analyzing polymorphism data in both species. Strong statistical evidence for hotspots of recombination was obtained in both species. Despite ~99% identity at the level of DNA sequence, however, recombination hotspots were found rarely (if at all) at the same positions in the two species, and no correlation was observed in estimates of fine-scale recombination rates. Thus, local patterns of recombination rate have evolved rapidly, in a manner disproportionate to the change in DNA sequence.

Recombination shapes genomic diversity, breaking up ancestral linkage disequilibrium (LD) and creating new combinations of alleles on which natural selection can act. As in yeast (*1*), recombination in the human genome principally occurs at so-called "hotspots" of recombination (*2*, *3*); experimentally characterized examples include the β-globin (*4*) and human leukocyte antigen (HLA) regions (*5*, *6*). Because direct observation of recombination hotspots is laborious, only with the recent development of statistical methods to estimate recombination rates from population genetic (polymorphism) data (*2*, *3*) has it become practical to study fine-scale recombination rates on a genomic scale.

The molecular determinants of hotspot location and activity are largely unknown. In yeast, chromatin structure influences initiation of double-strand breaks (DSBs) at hotspots (*7*). Directed mutagenesis of single nucleotides can disrupt hotspot activity (*8*), and different alleles of the same locus can show differences in recombination (*9*–*11*), indicating strong sequence specificity. However, no sequence motif has been identified as causing recombination hotspots. The observation of meiotic drive at hotspots has led to the hypothesis that hotspots